Available online at www.sciencedirect.com

ScienceDirect

Optics Communications 281 (2008) 3301–3313

Optics Communications

www.elsevier.com/locate/optcom

Tunable all-optical bistability in a semiconductor quantum dot damped by a phase-dependent reservoir

M.A. Antón *, F. Carreño, Oscar G. Calderón, Sonia Melle

Escuela Universitaria de Óptica, Universidad Complutense de Madrid, C/Arcos de Jalón s/n, 28037 Madrid, Spain

Received 18 December 2007; received in revised form 14 February 2008; accepted 22 February 2008

Abstract

We propose a method of frequency and phase control of optical bistability in a unidirectional ring cavity containing a semiconductor structure which is characterized as a ladder three-level system. The system interacts with a coherent probe field, and a control field which consists of a strong coherent field and a weak amplitude-fluctuating stochastic field. A perturbative solution of the master equation of the system allows to eliminate the stochastic field and provides a physical picture in terms of correlation properties of the stochastic field. We find that the bistable response can be modified strongly by means of the amplitude, the frequency and the phase of the stochastic field. In order to illustrate the feasibility of the results, we use parameter values corresponding to an semiconductor quantum dot (QD). This investigation may be used to optimize and control the optical switching process in the QD solid-state system, which is much more practical than that in atomic systems.

Keywords: Atomic coherence effects; Cooperative phenomena 40.040; 40.060

1. Introduction

Control of light by light is essential in all-optical communication and optical computing. In the past two decades, all-optical switches based on optical bistability (OB) in two-level atomic systems have been extensively studied [1–5]. Such optical bistable behavior arises from the nonlinear interaction between a collection of two-level atoms and the field inside an optical cavity. Many interesting phenomena in these OB systems such as dynamic instabilities, squeezed states, cavity QED, and higher order quantum correlation were all experimentally observed [6]. Later, Arecchi et al. included the effect of ground state coherence and reported not only tristability but also higher order bistability [7]. The tristability generated here involved a two-photon process via the cooperation of a bistability generation process. Several groups reported the observations of multistable/multiple hysteresis behaviors in a Fabry–Perot cavity filled with atoms having several degenerate or nearly degenerate sublevels in the ground state and driven by linearly polarized light [8].

In traditional systems, OB has a fundamental drawback for practical applications since the only controllable optical beam is the input field which, in turn, is part of the bistable curve in the input–output plot. The situation changes when we consider multilevel atoms inside a cavity. In this case there are new control fields between the different atomic levels and some of them do not circulate inside the cavity and, consequently, can be used for altering almost at will the bistable response. OB was explored in three-level atomic systems, in which multistable and unstable behaviors were observed. Optical multistability (OM) was predicted and observed in systems involving interactions between non-linear media and two different optical cavity field modes. In particular, Kitano et al. [9] predicted optical tristability in a three-level configuration under the limiting

* Corresponding author. Tel.: +34 913946855; fax: +34 913946885.
E-mail address: antonm@fis.ucm.es (M.A. Antón).

0030-4018/$ - see front matter © 2008 Elsevier B.V. All rights reserved.
doi:10.1016/j.optcom.2008.02.027

condition of large atomic detuning with no saturation, which was experimentally observed by Cecchi et al. [10]. Even more interestingly, new physical mechanisms such as quantum interference and coherence effects, which can greatly modify the absorption, dispersion and non-linearity of the system, can be exploited to engineer the OB in these atomic schema. In earlier works, Walls et al. [11,12] proposed a novel scheme for OB by using atomic coherence effects in three-level Λ-type atoms, and similar studies were carried out in a ladder system by Harshawardhan et al. [13]. OB in such multilevel atoms was found to be originated by population trapping in a coherent superposition of the ground state sublevels. The main feature of this mechanism relies on the fact that it does not require atomic saturation, thus OB is achieved with low laser intensities compared to those required in previously considered atomic schema. From an experimental point of view, OB in three-level systems based in electromagnetically induced coherence has been investigated extensively by Xiao and coworkers in a system consisting of three-level rubidium atoms in an optical ring cavity. They presented a demonstration of controlling the cavity output intensity of one laser beam with the intensity of another laser beam. In a series of successfully papers they have shown the quantum coherence effects in three-level Λ-type atoms such as cavity-linewidth narrowing [14]. Optical bistability and instability were experimentally observed and manipulated by changing the control and cavity field parameters [15,16]. Joshi et al. [17–19] have explored their preliminary observations in [16] to show the dependence of the OB on various parameters such as intensity and frequency detuning of the coupling field. Four level atomic systems have also been explored showing interesting features. For example, Chang et al. [20] have observed controllable shift of the threshold points and the hysteresis curve of OB induced by two suitable tuned fields. All-optical flip-flop and storage of optical signals were obtained by controlling this shift. Similar behavior has been analyzed in a tripod four level atom in [21]. A novel form of non-linearity, i.e., dynamic optical bistability, has been demonstrated in resonantly enhanced stimulated Raman scattering by Novikova et al. [22]. Joshi et al. [23] have extended this behavior in a three-level Λ-type atom by changing the sweeping frequency of the cavity input field in the optical bistability response of rubidium atoms. Finally, it is worth noting that other ways of generating coherence connected with the relaxation processes such as spontaneous emission have been reported in three-level Λ-type atoms [24]. Similar studies have been carried out in V-type atoms driven by a coherent field in a broadband squeezed vacuum taking into account the possibility of quantum interference between the two decay channels from the two upper sublevels to the ground level [25,26]. It is found that OB can be achieved with considerable lower threshold intensity to the width of the hysteresis loop can be controlled by the relative phase of the squeezed vacuum to the coherent field. Others different mechanisms to realize OB have appeared by using atomic coherence, for example, via initial coherence of atoms [27], or via microwave field induced coherence [28].

While most of quantum-coherence experiments involve dilute systems, there is also interest in obtaining similar effects in semiconductors. Such obtention may produce a potentially drastic increase in practical applications because the widespread use of semiconductors components in optoelectronics to obtain optical tunable delay lines, buffers, quantum switches, among others. Devices which take advantage of intersubband transitions in quantum wells (QW's) and quantum dots (QD's) have inherent advantages, such as large electric dipole moments due to the small effective electron mass, and a great flexibility in the device design by a proper selection of the materials and their sizes. Quantum coherence and interference phenomena have been studied theoretically and experimentally in intersubband transitions in the conduction band of semiconductor QW's and QD's [29–31]. In particular, electromagnetically induced transparency (EIT) was experimentally obtained using exciton and biexciton transitions in a QW structure [32–35]. There are additional studies on laser without inversion (LWI), refractive index enhancement in semiconductor nano-structures for coherent mid-to far-infrared radiation generation [36], optical storage [37,38], and for sensitive infrared detectors [39]. In addition, extremely useful devices such as ultrafast optical switches [40–42] operating at hundreds of GHz, and quantum switches [43] based on Fano-type interferences in double QW's operating at low intensities have been reported. In these systems the coherence is established by resonant tunneling which enables one to change the coupling strength with a bias voltage. Another mechanism which relies on the establishment of an initial coherence has also been explored to obtain EIT in these systems. In particular, Pötz [44] studied coherent control in intersubband transitions by using the phase difference between a pump pulse and a control pulse, and he found that gain can be achieved by changing the relative phase of two pump fields. At the same time, some attempts have appeared in order to explore OB phenomena based on electromagnetically induced coherence in semiconductors. Joshi and Xiao [45] have theoretically demonstrated the possibility of observing OB in a system consisting in InGaAs QW with AlInAs barriers which was modeled as a three-level system in a ladder configuration and driven by a strong field under two-photon resonant condition. Li has analyzed OB via tunable Fano interferences based on intersubband transitions using three and four atom-like models [46,47]. All these effects are very sensitive to the detuning between the driving field and the optical transitions (two-photon resonance), so a perfect tuning between the driving fields and the atomic transitions involved must be fulfilled. It is well-known that any perturbation of this condition will dramatically modify the absorptive and dispersive properties of the system. In view of this, the main motivation of this paper is to explore the possibility of controlling the bistable response by means of a weak amplitude-fluctuating field superimposed to a coherent control field in these kind of systems. We remind here that the atomic response to a fluctuating field has been a subject of previous consideration. The first discussion of the effects of statistical fluctuations upon OB was apparently in [48]. In the case of absorptive optical bistability, the simplest model which describes amplitude fluctuations in this system is given by a Langevin equation with additive noise [49,50]. Using a more phenomenological approach, Hanggi et al. [51] derived Ito stochastic differential equation for the amplitude fluctuation with multiplicative Gaussian white noise to describe the OB system in the good cavity limit. Recently phase fluctuation effects on the absorptive optical bistability in a two-level system have been studied [52,53] and a very peculiar phenomenon is shown, namely when the cooperativity parameter $C < 4$, noise still can induce optical bistability. The phenomenon of noise-induced optical bistability in this paper is just the example of noise-induced phase transition. In addition, Zhou and Swain [54] have pointed out that in a two-level atom driven by a strong coherent field as well as a weak stochastic field with wide bandwidth, the stochastic field can give rise to phase-sensitive spectral profiles in resonance florescence similar to those which occur when the atom is damped by a broadband squeezed vacuum. On the context of OB in three-level systems, Gong et al. [55] and Antón and Calderón [25] showed that phase fluctuations of the control field may alter the bistable response. Hu et al. [56] and Osman and Hassan [57] also showed that in three-level Λ-type atoms, OB can be achieved via amplitude-fluctuating fields. In these works both the control and stochastic fields are considered to have the same angular frequency. In this work we will study the dependence of input–output bistable response on several parameters and we will address a general situation where the angular frequencies of the control and stochastic fields differ each other. Moreover, we will show that the probe field must be taken into account in order to properly obtain the bistable response in the regime of high Rabi frequencies of the probe field. Specifically, we investigate the behavior of a probe field in a unidirectional ring cavity containing a semiconductor QD similar to that studied in the context of obtaining slow-light [58–60].

The paper is organized as follows: in Section 2 we derive an effective master equation for the reduced density operator beyond the weak-probe field approximation by adiabatically eliminating the stochastic field variables when the coherent control field is stronger than the stochastic part. Section 3 deals with Maxwell's equation in a ring cavity and presents numerical simulations illustrating the influence of the stochastic field in the bistable response of the system. It is shown that dynamical control of the bistable response of the system may be achieved by adjusting the frequency and phase of the stochastic field which allows for multistability. The main conclusions are summarized in Section 4.

2. The model

In order to model the study of OB in a quantum dot (QD) we consider a InAs QD embedded in GaAs. QD are zero-dimensional systems where the electrons are confined in the three dimensions of space. Therefore, all the bound states of the dot are discrete levels and in some way, QD's behave like atoms, but unlike atoms, their properties can be artificially designed. Fig. 1 depicts the energy-level diagram of the InAs quantum dot structure. The level $|1\rangle$ represents the ground state of the valence band, whereas $|2\rangle$ and $|3\rangle$ are the first excited states of the conduction band. The separation energies are $E_{21} = 636$ meV and $E_{32} = 145$ meV. Let ω_{21} and ω_{32} be the frequencies of the $|1\rangle \rightarrow |2\rangle$ and $|2\rangle \rightarrow |3\rangle$ transitions, respectively. A strong coupling beam excites the intersubband transition $|2\rangle \leftrightarrow |3\rangle$, thereby producing a change in the susceptibility experienced by a probe signal tuned close to the interband transition $|1\rangle \leftrightarrow |2\rangle$. This kind of structures have been already studied in the context of obtaining slow-light [58,59] and pulse propagation in the EIT regime [60].

We write the total electric field as

$$E(z,t) = E_c(z,t) + E_s(z,t) + E_p(z,t). \tag{1}$$

Here we consider that transition $|2\rangle \leftrightarrow |3\rangle$ is driven by a coherent field given by

$$E_c(z,t) = \frac{1}{2} E_{c0} e^{-ih(\omega_c t - kz + \phi_c)} + \text{c.c.}, \tag{2}$$

where E_{c0}, ω_c, and ϕ_c are the amplitude, frequency, and phase of the control field, respectively. Superimposed to the coherent control field, there is a weak amplitude-fluctuating field which couples the same transition $|2\rangle \rightarrow |3\rangle$. The fluctuating field is described by the expression

$$E_s(z,t) = \frac{1}{2} E_{s0}(t) e^{-i(\omega_s t - kz + \phi_s)} + \text{c.c.}, \tag{3}$$

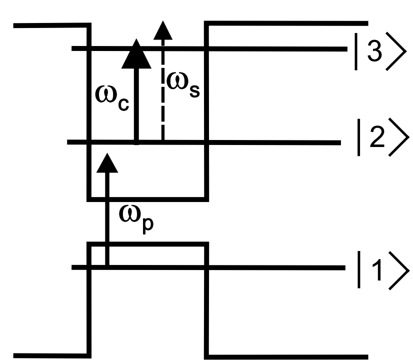

Fig. 1. Schematic representation of the QD. Level $|1\rangle$ represents the ground state, and $|2\rangle$ and $|3\rangle$ are the subband excited states. The probe laser interacts with subband transition $|1\rangle \rightarrow |2\rangle$, while the control laser acts on subband transition $|2\rangle \rightarrow |3\rangle$. The control laser consists of two parts: a coherent field and a stochastic field with angular frequencies ω_c and ω_s, respectively.

where $E_{s0}(t)$, ω_s, and ϕ_s are the amplitude, the frequency, and the phase of the stochastic field, respectively. Note that we consider that ω_s may be different to ω_c.

The system is probed by a field which connects the $|1\rangle \to |2\rangle$ transition

$$E_p(z,t) = \frac{1}{2}E_{p0}e^{-i(\omega_p t - kz + \phi_p)} + \text{c.c.}, \tag{4}$$

where E_{p0}, ω_p and ϕ_p are the amplitude, frequency and phase of the probe field, respectively.

Several theoretical and experimental studies devoted to electromagnetically induced coherence in semiconductor nanostructures have appeared recently for coherent mid- to far-infrared radiation generation [36] and optical storage and slow light [37]. There, steady-state results are obtained by assuming that a semiconductor system behaves analogous to an inhomogeneously broadened atomic system with strong dephasing effects. This approach has allowed to successfully address many analogies such as the excitonic optical Stark effect and excitonic Rabi oscillations. However there are two major differences, one being the significantly faster dephasing processes in the order of femtoseconds to picoseconds [61], instead of microseconds as in an atomic system. The second difference is that one can no longer assume to have an isolated three-level atom. This three-level QD will be energetically in close proximity to other quantum dot bound states and to a continuum comprising states from the quantum well embedding the quantum dots. The Coulomb interaction couples discrete and continuum states, resulting in collision-induced carrier-population redistribution, as well as many-body energy and field renormalizations [62].

In the analysis carried out in this paper, we assume a situation in which optical excitation is not too strong, so the effect of bandgap renormalization can be neglected. Therefore, from the Coulomb interaction we only keep the mutual attraction between electrons and holes. This approximation is justified if the density of generated electron–hole pairs is well below the Mott density [63]. In this case, we assume that the system may be described by using the density matrix formalism in a way that mimics a ladder-type three-level atomic system. This approach has described quantitatively the results of several experimental papers [34,35,38,39,42]. The effective Hamiltonian can be expressed as (see Eq. (A.14) in Appendix A for more details):

$$\begin{aligned} H^c_{\text{eff}} &= \hbar\left[\Delta_p\sigma_{22} + (\Delta_p + \Delta_c)\sigma_{33}\right] - \hbar\left(\Omega_p\sigma_{21} + \Omega_c\sigma_{32} + \text{H.c.}\right), \\ H_s(t) &= -\hbar\left(G_s(t)e^{i(\delta_s t + \phi)}\sigma_{32} + \text{H.c.}\right), \end{aligned} \tag{5}$$

where $\Delta_p = \omega_{21} - \omega_p$, and $\Delta_c = \omega_{32} - \omega_c$, denote the probe and control field detunings, respectively. The atomic operators σ_{ij} are defined as $\sigma_{ij} = |i\rangle\langle j|$, where $|i\rangle$ and $|j\rangle$ stand for levels $|1\rangle$,$|2\rangle$, or $|3\rangle$. The corresponding Rabi frequencies in the probe, control, and stochastic field are given by $\Omega_p = \mu_{21}E_{p0}/2\hbar$, $\Omega_c = \mu_{32}E_{c0}/2\hbar$, and $G_s(t) = \mu_{32}E_{s0}(t)/2\hbar$, respectively. μ_{21} and μ_{32} represent the dipole moments of the transitions involved. Finally $\delta_s = (\omega_s - \omega_c)$, and $\phi = \phi_s - \phi_c$, are the frequency detuning and the relative phase between the stochastic field and the control field, respectively.

We can write the equation of motion for the reduced density matrix in the interaction picture and in the rotating wave approximation as

$$\frac{\partial\rho}{\partial t} = -\frac{i}{\hbar}\left[H^c_{\text{eff}} + H_s(t), \rho\right] + \left(\frac{\partial\rho}{\partial t}\right)_{\text{deph}}, \tag{6}$$

where H^c_{eff} is the effective Hamiltonian corresponding to coherent fields, $H_s(t)$ is the Hamiltonian associated to the stochastic field and $(\frac{\partial\rho}{\partial t})_{\text{deph}}$ represents the collision contributions described in Appendix A. The dephasing processes enter in this model, via the population decay γ_i^{dph} and the transition dephasing parameters γ_{ij}^{dph} (see Appendix A). In contrast to isolated atoms where both processes are determined by radiative coupling to isotropic photon modes, in QD are determined by coupling to the lattice phonon spectrum, electron–electron interaction, interface roughness and photon scattering processes. Inhomogeneous broadening arising from fluctuations in the QD size is not taken into account. A more realistic model would include such fluctuations. Nevertheless, the present model can provide a good illustration of the optical processes of interest.

We assume that the amplitude fluctuations have the properties of a real Gaussian Markovian random process with zero mean value and correlation function [54] given by

$$\langle G_s(t)G_s(t')\rangle = D\kappa e^{-\kappa|t-t'|}. \tag{7}$$

This correlation function describes a field undergoing amplitude fluctuations which results in a finite bandwidth κ of the field with a Lorentzian spectral profile, 2κ being its width and D the strength of the stochastic process.

The master Eq. (6) leads to a set of stochastic equations because of the nature of the Langevin amplitude fluctuations of the field $G_s(t)$. They can be solved numerically using Monte Carlo simulation methods. However, in order to obtain analytical results, we resort to eliminate the stochastic variable $G_s(t)$ by using standard perturbative techniques [64]. Thus, we assume that the correlation time κ^{-1} of the stochastic field is very short compared to the radiative lifetimes $\gamma_i^{-1} (i = 2, 3)$ of the atomic transitions. We also consider that the intensity of the coherent field is much greater than that of the stochastic field, that is, that the following conditions hold

$$\begin{aligned} &\kappa \gg \gamma_2, \gamma_3, \\ &\Omega_c \gg \sqrt{D\kappa}. \end{aligned} \tag{8}$$

In view of the previous considerations, the QD experiences always the fluctuating field in a state induced by the coherent fields, and this allows us to eliminate the variables containing the stochastic field operators adiabatically [64]. This gives rise to a reduced master equation for the coherent variables only. The derivation is tedious but straightforward, so we here outline only the key points. First, we perform a canonical transformation to the QD interaction picture by considering $H_{\mathrm{eff}}^{\mathrm{c}}$ in Eq. (5), which reads as

$$\rho_{\mathrm{N}} = \mathrm{e}^{\mathrm{i}H_{\mathrm{eff}}^{\mathrm{c}}t}\rho\mathrm{e}^{-\mathrm{i}H_{\mathrm{eff}}^{\mathrm{c}}t}. \tag{9}$$

In this picture, the master equation (6) can be written as

$$\frac{\mathrm{d}\rho_{\mathrm{N}}}{\mathrm{d}t} = -\frac{\mathrm{i}}{\hbar}\left[H_{\mathrm{s}}^{(N)}(t),\rho_{\mathrm{N}}\right] + \mathrm{e}^{\mathrm{i}H_{\mathrm{eff}}^{\mathrm{c}}t}\left(\frac{\partial\rho}{\partial t}\right)_{\mathrm{deph}}\mathrm{e}^{-\mathrm{i}H_{\mathrm{eff}}^{\mathrm{c}}t}, \tag{10}$$

where $H_{\mathrm{s}}^{(\mathrm{N})}$ is given by $H_{\mathrm{s}}^{(\mathrm{N})} = \mathrm{e}^{\mathrm{i}H_{\mathrm{eff}}^{\mathrm{c}}t}; H_{\mathrm{s}}\rho\mathrm{e}^{-\mathrm{i}H_{\mathrm{eff}}^{\mathrm{c}}t}$.

Now we can perform a second-order perturbation calculation with respect to $D\kappa$ which produces the following master equation:

$$\begin{aligned}\frac{\mathrm{d}\rho_{\mathrm{N}}}{\mathrm{d}t} = &-\frac{i}{\hbar}\left[H_{\mathrm{s}}^{(\mathrm{N})}(t),\rho_{\mathrm{N}}(t)\right] - \frac{1}{\hbar^2}\\ &\times\int_0^\infty \left[H_{\mathrm{s}}^{(\mathrm{N})}(t),\left[H_{\mathrm{s}}^{(\mathrm{N})}(t'),\rho_{\mathrm{N}}(t')\right]\right]\mathrm{d}t'\\ &+\mathrm{e}^{\mathrm{i}H_{\mathrm{eff}}^{\mathrm{c}}t}\left(\frac{\partial\rho}{\partial t}\right)_{\mathrm{deph}}\mathrm{e}^{-\mathrm{i}H_{\mathrm{eff}}^{\mathrm{c}}t}.\end{aligned} \tag{11}$$

At this time we perform the trace to Eq. (11), we invoke the Born–Markov approximation and take into account the correlation properties of the stochastic field [see Eq. (7)]. The result (ρ_{N}) is transformed back to the original picture via $\rho = \mathrm{e}^{-\mathrm{i}H_{\mathrm{eff}}^{\mathrm{c}}t}\rho_{\mathrm{N}}\mathrm{e}^{\mathrm{i}H_{\mathrm{eff}}^{\mathrm{c}}t}$, and we obtain the following master equation:

$$\begin{aligned}\frac{\mathrm{d}\rho}{\mathrm{d}t} = &-\frac{\mathrm{i}}{\hbar}\left[H_{\mathrm{eff}}^{\mathrm{c}},\rho\right] + \left(\frac{\partial\rho}{\partial t}\right)_{\mathrm{deph}} + [\sigma_{32},[S_+,\rho]]\mathrm{e}^{\mathrm{i}(2\delta_{\mathrm{s}}t+2\phi)}\\ &+[\sigma_{23},[S_-,\rho]]\mathrm{e}^{-\mathrm{i}(2\delta_{\mathrm{s}}t+2\phi)} + [\sigma_{23},[S_+,\rho]]\\ &+[\sigma_{32},[S_-,\rho]],\end{aligned} \tag{12}$$

where

$$S_+ = D\kappa\int_0^\infty \mathrm{d}\tau\mathrm{e}^{-(\kappa+\mathrm{i}\delta_{\mathrm{s}})\tau}\mathrm{e}^{-\mathrm{i}H_{\mathrm{eff}}^{\mathrm{c}}\tau}\sigma_{32}\mathrm{e}^{\mathrm{i}H_{\mathrm{eff}}^{\mathrm{c}}\tau}, \tag{13}$$

and $S_- = (S_+)^\dagger$. The first term of Eq. (12) describes the interaction of the atomic system with the coherent fields Ω_{p} and Ω_{c}. The second term is the vacuum induced incoherent decay of the QD while the rest of the terms are associated with the effect of the stochastic field and consist of incoherent decays and pumpings.

In order to carry out the unitary transformation $\mathrm{e}^{-\mathrm{i}H_{\mathrm{eff}}^{\mathrm{c}}\tau}\sigma_{32}\mathrm{e}^{\mathrm{i}H_{\mathrm{eff}}^{\mathrm{c}}\tau}$ appearing under the integral in Eq. (13), it is very convenient to express $H_{\mathrm{eff}}^{\mathrm{c}}$ and σ_{32} in the dressed basis of $H_{\mathrm{eff}}^{\mathrm{c}}$. In this basis the operator $H_{\mathrm{eff}}^{\mathrm{c}}$ becomes diagonal and the unitary transformation can be easily accomplished, which allows to express S_+ in terms of the atomic operators in the dressed basis where the integral is straightforward. The results are then inverted to obtain S_+ in the bare basis. In related works [56,57], this process was carried out by diagonalizing the Hamiltonian corresponding only to the coherent control field and then assuming that $\Omega_{\mathrm{p}} \ll \Omega_{\mathrm{c}}$, thus to evaluate S_+, $H_{\mathrm{eff}}^{\mathrm{c}}$ appearing in Eq. (13) was restricted to the following expression

$$H_0^{\mathrm{c}} = \hbar\left[\Delta_{\mathrm{p}}\sigma_{22} + (\Delta_{\mathrm{p}}+\Delta_{\mathrm{c}})\sigma_{33}\right] - \hbar(\Omega_{\mathrm{c}}\sigma_{32} + \mathrm{H.c.}), \tag{14}$$

and the eigenvalue problem was

$$H_0^{\mathrm{c}}|\psi\rangle = \hbar\lambda_i|\psi\rangle, (i=1,2), \tag{15}$$

where $|\psi\rangle = c_{i1}|1\rangle + c_{i2}|2\rangle + \ c_{i3}|3\rangle$. This procedure could work well when, for example, one is interested in analyzing the absorption of a weak probe field which experiences the atom as dressed by the strong control field. But in non-linear phenomena such as OB, the very probe field can reach considerable high values inside the cavity, so, in order to focus attention on the change in the response of the atomic system as the strength of the probe field is increased, all the terms of the coherent Hamiltonian ($H_{\mathrm{eff}}^{\mathrm{c}}$) must be considered to obtain the dressed states. Thus, in this work we resort to find the eigenvalues and eigenstates of the full atomic plus the coherent part of the hamiltonian $H_{\mathrm{eff}}^{\mathrm{c}}$ as given by Eq. (5). The dressed states are labelled $|\alpha\rangle$,$|\beta\rangle$ and $|\gamma\rangle$ and can be written in terms of the bare states $|1\rangle$,$|2\rangle$ and $|3\rangle$ as

$$\begin{pmatrix}|\alpha\rangle\\|\beta\rangle\\|\gamma\rangle\end{pmatrix} = \begin{pmatrix}a_{1\alpha} & a_{2\alpha} & a_{3\alpha}\\ a_{1\beta} & a_{2\beta} & a_{3\beta}\\ a_{1\gamma} & a_{2\gamma} & a_{3\gamma}\end{pmatrix}\begin{pmatrix}|1\rangle\\|2\rangle\\|3\rangle\end{pmatrix}, \tag{16}$$

where the coefficients are explicitly given by

$$\begin{aligned}a_{1j} &= \frac{|\lambda_j|\Omega_{\mathrm{p}}\Omega_{\mathrm{c}}}{\lambda_j D_j},\\ a_{2j} &= \frac{|\lambda_j|\Omega_{\mathrm{c}}}{D_j},\\ a_{3j} &= \frac{|\lambda_j|\left[(\Delta_{\mathrm{p}}-\lambda_j)\lambda_j - \Omega_{\mathrm{p}}^2)\right]}{\lambda_j D_j},\end{aligned} \tag{17}$$

with $D_j = \sqrt{(\lambda_j^2+\Omega_{\mathrm{p}}^2)\Omega_{\mathrm{c}}^2 + [(\Delta_{\mathrm{p}}-\lambda_j)\lambda_j - \Omega_{\mathrm{p}}^2]^2}(j=\alpha,\beta,\gamma)$. The eigenvalues λ_j are the roots of the cubic equation

$$\begin{aligned}&\lambda^3 - (2\Delta_{\mathrm{p}}+\Delta_{\mathrm{c}})\lambda^2 + \left[\Delta_{\mathrm{p}}(\Delta_{\mathrm{p}}+\Delta_{\mathrm{c}}) - (\Omega_{\mathrm{p}}^2+\Omega_{\mathrm{c}}^2)\right]\lambda\\ &\quad + \Omega_{\mathrm{p}}^2(\Delta_{\mathrm{p}}+\Delta_{\mathrm{c}}) = 0.\end{aligned} \tag{18}$$

With this in mind, the operator S_+ given in Eq. (13) can be expressed as

$$\begin{aligned}S_+ &= D\kappa\int_0^\infty \mathrm{d}\tau\mathrm{e}^{-(\kappa+\mathrm{i}\delta_{\mathrm{s}})\tau}\mathrm{e}^{-\mathrm{i}H_0\tau}\sigma_{32}\mathrm{e}^{\mathrm{i}H_0\tau}\\ &= \beta_1\sigma_{11} + \beta_2\sigma_{22} + \beta_3\sigma_{33} + \beta_4\sigma_{32} + \beta_5\sigma_{23} + \beta_6\sigma_{12}\\ &\quad + \beta_7\sigma_{21} + \beta_8\sigma_{13} + \beta_9\sigma_{31}.\end{aligned} \tag{19}$$

The coefficients $\beta_i(i=1,\dots,9)$ are obtained from the following expression

$$\vec{\beta} = M\vec{\gamma}, \tag{20}$$

where $\vec{\beta}$ is a vector defined as $\vec{\beta} \equiv [\beta_1,\beta_2,\beta_3,\dots\beta_9]^{\mathrm{tt}}$, tt being a label to indicate the transpose operation, and $\vec{\gamma}$ is the following vector

$$\vec{\gamma} \equiv \begin{pmatrix} 1/(\kappa + i\delta_s) \\ 1/(\kappa + i[\delta_s + (\lambda_\gamma - \lambda_\alpha)]) \\ 1/(\kappa + i[\delta_s + (\lambda_\gamma - \lambda_\beta)]) \\ 1/(\kappa + i[\delta_s + (\lambda_\beta - \lambda_\alpha)]) \\ 1/(\kappa + i[\delta_s + (\lambda_\alpha - \lambda_\beta)]) \\ 1/(\kappa + i[\delta_s + (\lambda_\alpha - \lambda_\gamma)]) \\ 1/(\kappa + i[\delta_s + (\lambda_\beta - \lambda_\gamma)]) \end{pmatrix}. \tag{21}$$

M appearing in Eq. (20) is a 9×7 matrix and may be expressed in terms of the coefficients a_{ij} ($i = 1,2,3$, $j = \alpha,\beta,\gamma$) given in Eq. (17) (see Appendix B for more details). It is clear from Eq. (20) that the coefficients β_i are frequency dependent and resonant when the central frequency of the stochastic field is tuned to $\delta_s = (0, \lambda_i \pm \lambda_j)$. Thus, if the frequency of the stochastic field is properly detuned from the intersubband transition of the QD, the corresponding dressed transition can be enhanced to the absorptive and dispersive properties of the system will change. This fact will be exploited to adjust the OB response of this system.

From the atomic master equation given in Eq. (12), we can obtain the Bloch equations for the density matrix elements including atomic spontaneous emission and dephasing

$$\begin{aligned}
\frac{\partial\rho_{31}}{\partial t} &= -\left[\frac{\gamma_{31}}{2} + i(\varDelta_p + \varDelta_c) + \beta_5 e^{i2\psi}\right]\rho_{31} \\
&\quad + \left[i\Omega_c - (\beta_2 - \beta_1)e^{i2\psi}\right]\rho_{21} \\
&\quad - (\beta_9^* e^{i2\psi} + i\Omega_p)\rho_{32} - \beta_9 e^{-i2\psi}\rho_{23} \\
&\quad - (\beta_2^* - \beta_1^*)e^{-i2\psi}\rho_{12} - \beta_5^* e^{-i2\psi}\rho_{13} \\
&\quad - (\rho_{11} - \rho_{22})(\beta_7 e^{i2\psi} + \beta_7^* e^{-i2\psi}), \\
\frac{\partial\rho_{32}}{\partial t} &= -\left[\frac{\gamma_{32}}{2} + i\varDelta_c + 2(\beta_5 e^{i2\psi} - \beta_4^* e^{-i2\psi})\right]\rho_{32} \\
&\quad + i\Omega_c(\rho_{22} - \rho_{33}) + (\beta_9^* e^{-i2\psi} - \beta_8 e^{i2\psi})\rho_{31} \\
&\quad + (\beta_6 e^{i2\psi} - \beta_7^* e^{-i2\psi})\rho_{21} + (\beta_6^* e^{-i2\psi} - \beta_7 e^{-i2\psi})\rho_{12} \\
&\quad + 2(\beta_4 e^{i2\psi} - \beta_5^* e^{-i2\psi})\rho_{23} + (\beta_9 e^{i2\psi} - \beta_8^* e^{-i2\psi})\rho_{13}, \\
\frac{\partial\rho_{21}}{\partial t} &= -\left[\frac{\gamma_{21}}{2} + i\varDelta_p + \beta_4\right]\rho_{21} + (i\Omega_p + \beta_9 + \beta_9^*)(\rho_{11} - \rho_{22}) \\
&\quad + \left[i\Omega_c^* - (\beta_3 - \beta_1)\right]\rho_{31} - (\beta_3^* - \beta_1^*)\rho_{13} - \beta_4^*\rho_{12} \\
&\quad + \beta_7\rho_{32} + \beta_7^*\rho_{23}, \\
\frac{\partial\rho_{33}}{\partial t} &= -\left[\gamma_3 + (\beta_5 e^{i2\psi} + \beta_5^* e^{-i2\psi}) + \beta_4 + \beta_4^*\right]\rho_{33} \\
&\quad + \left[\beta_5 e^{i2\psi} + \beta_5^* e^{-i2\psi} + \beta_4 + \beta_4^*\right]\rho_{22} \\
&\quad - \left[i\Omega_c^* + (\beta_2^* - \beta_3^*)e^{-i2\psi} + (\beta_2 - \beta_3)\right]\rho_{32} \\
&\quad + \left[i\Omega_c - (\beta_2 - \beta_3)e^{i2\psi} - (\beta_2^* - \beta_3^*)\right]\rho_{23} \\
&\quad - (\beta_7^* e^{-i2\psi} + \beta_6)\rho_{31} - (\beta_7 e^{i2\psi} + \beta_6^*)\rho_{13} \\
&\quad + (\beta_8 e^{i2\psi} + \beta_9^*)\rho_{21} + (\beta_8^* e^{-i2\psi} + \beta_9)\rho_{12}, \\
\frac{\partial\rho_{22}}{\partial t} &= -\left[\gamma_2 + (\beta_5 e^{i2\psi} + \beta_5^* e^{-i2\psi}) + \beta_4 + \beta_4^*\right]\rho_{22} \\
&\quad + \left[\gamma_3 + (\beta_5 e^{i2\psi} + \beta_5^* e^{-i2\psi}) + \beta_4 + \beta_4^*\right]\rho_{33} \\
&\quad + \left[i\Omega_c^* - (\beta_3^* - \beta_2^*)e^{-i2\psi} - (\beta_3 - \beta_2)\right]\rho_{32} \\
&\quad - \left[i\Omega_c + (\beta_3 - \beta_2)e^{i2\psi} + (\beta_3^* - \beta_2^*)\right]\rho_{23} \\
&\quad + (i\Omega_p - \beta_8^* e^{-i2\psi} - \beta_9)\rho_{12} \\
&\quad - (i\Omega_p^* + \beta_8 e^{i2\psi} + \beta_9^*)\rho_{21},
\end{aligned} \tag{22}$$

where $\psi = \delta_s t + \phi$, and the coherence relaxations are γ_{31}, γ_{21}, and γ_{32}. Dephasing rates for semiconductors usually ranges from μeV at very low temperatures to meV at room temperature [61], thus the influence of dephasing on the atomic response is of major interest. In order to evaluate the feasibility of this approach, we consider the dephasing parameters based in experimental results for a similar QD, namely, $\gamma_2 = \gamma_3 = \gamma_{32} = \gamma_{12} = \gamma_{13} = 4.13$ μeV [61].

The equations for ρ_{12},ρ_{13}, and ρ_{23} can be obtained from Eq. (22) by complex conjugation, and because of the closing condition $\rho_{11} + \rho_{22} + \rho_{33} = 1$, Eq. (22) generates a set of eight linearly independent equations. It is worth noting that a phase-dependent term appears which oscillates at $2\delta_s t$. Obviously, for $\delta_s \neq 0$, this term averages to zero, but it becomes relevant when the frequency of the stochastic field is equal to that of the control coherent field. In this case, the equations reveal an interesting dependence on the phase $\phi = \phi_s - \phi_c$, i.e., the difference between the phase of the stochastic field to the phase of the control field. In addition, the stochastic field modifies the dephasing terms of the coherences in Eq. (22) and more interestingly, it couples ρ_{21} not only with ρ_{31}, as usual, but also with ρ_{12} and ρ_{13}, which dephases the atomic coherence and changes the absorptive properties. It is worth mentioning that under special circumstances this kind of coupling resembles that produced by a squeezed reservoir [54].

3. Effect of the stochastic field on the bistable response

In order to study the role of the stochastic field on the bistable response in the semiconductor system, let us consider a structure of length L_c composed by a collection of QD's inserted in a unidirectional ring cavity (see Fig. 2). The propagation of the laser field in the medium is governed by Maxwell's wave equation, which in the slowly varying envelope approximation reduces to

$$c\frac{\partial E(z,t)}{\partial z} + \frac{\partial E(z,t)}{\partial t} = i\frac{\omega_p}{\epsilon_0}P(\omega_p), \tag{23}$$

where $P(\omega_p)$ is the slowly oscillating term of the induced polarization

$$P(\omega_p) = N_c\mu_{21}\rho_{21}, \tag{24}$$

N_c being the electron density in the conduction band of the QD. For a perfectly tuned cavity, the boundary conditions in the steady-state limit are given by [1]:

$$E_p(0) = \sqrt{T}E_{IP} + RE_p(L), \tag{25}$$

$$E_{TP} = \sqrt{T}E_p(L), \tag{26}$$

where R and T are the reflectance and the transmittance of the semi-silvered mirrors (see Fig. 2), and E_{IP} and E_{TP} are the incident and the transmitted fields, respectively. Using the boundary conditions (25)-(26) we obtain the mean-field state equation

$$\frac{\partial \Omega_{\mathrm{p}}(t)}{\partial t} = \bar{\kappa}\left[\Omega_{\mathrm{pI}} - \Omega_{\mathrm{p}}(t) + \mathrm{i}\gamma_2 C \rho_{21}\right], \tag{27}$$

where $\bar{\kappa} = cT/L_{\mathrm{c}}$ is the cavity decay rate, $\Omega_{\mathrm{p}} = \mu_{21}E_{\mathrm{p}}/2\hbar$ is the Rabi frequency of the cavity field, $\Omega_{\mathrm{pI}} = \mu_{21}E_{\mathrm{IP}}/2\hbar\sqrt{T}$ is the Rabi frequency of the incident field, and C is the cooperation parameter defined as usual (see Ref. [1])

$$C \equiv \frac{\mu_{21}^2 \omega_{21} N_{\mathrm{c}} L_{\mathrm{c}}}{2\hbar\gamma_2\epsilon_0 cT}. \tag{28}$$

Let's focus on the steady-state regime of the matter-radiation system, that is, we set the derivatives of Eqs. (22) and (27) equal to zero, and evaluate the steady-state of the transmitted field which is given by

$$y = x\left(1 + C\frac{\mathrm{Im}(\rho_{21})}{x}\right), \tag{29}$$

where we have defined the dimensionless incident and transmitted Rabi frequencies as $y \equiv \Omega_{\mathrm{pI}}/\gamma_2$ and $x \equiv \Omega_{\mathrm{p}}/\gamma_2$, respectively. From now on we numerically analyze the steady-state of the output field intensity versus the input field intensity in order to show the controllability of OB by changing the different parameters characterizing the stochastic field. In all numerical simulations we maintain the two-photon resonance condition by keeping $\Delta_{\mathrm{p}} + \Delta_{\mathrm{c}} = 0$. We also consider $C = 4 \times 10^3$, and $\kappa = 10\gamma_2$. The values of the strength of the stochastic field D and the Rabi frequency of the control field Ω_{c} are chosen to guarantee that condition (8) is satisfied. First of all, we will analyze the influence of the relative phase of the control field to the stochastic field ϕ. This situation arises when the central frequency of the coherent control field is adjusted to be equal to that of the stochastic field ($\delta_{\mathrm{s}} = 0$). Note that in this case the terms in the master equations where ϕ appears must be retained. This is an indication that the system can exhibit phase-

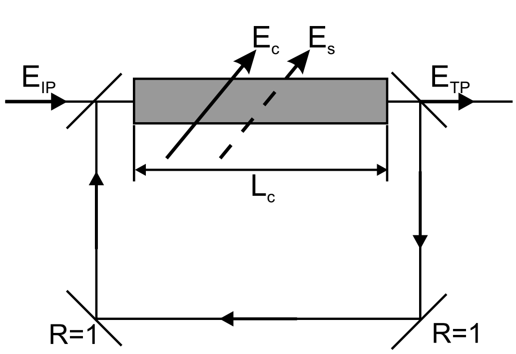

Fig. 2. Unidirectional ring cavity with the QD structure of length L_{c}. E_{IP} and E_{TP} are the incident and transmitted fields, respectively. E_{c} and E_{s} represent the injected control and stochastic fields, respectively.

dependent properties, thus it is expected that OB can be modified by acting on ϕ. The results are presented in Fig. 3a for several values of ϕ. In this case the input–output curves obtained for several values of the phase difference are modified when ϕ is changed in the following sense: the lower branch of the bistability curve remains essentially unaltered as ϕ changes, except for a minor change in the bistability threshold. However, at certain value of ϕ the upper branch is broken into several additional branches, i.e., multistability appears. This result contrast with other previously reported in other three-level schema where the variation of ϕ only induces the decrease of the bistability threshold [56] or even the appearance of bistability [57].

Multistability as shown with dashed-dotted line in Fig. 3a appears as a result of the action of both the control field (Ω_{c}) and the probe field (Ω_{p}): these two fields produce dressed states whose energy separation are modified by the probe field, since eigenvalues λ_i's are Ω_{p}-dependent [see Eq. (18)]. It is worth to stress how the evaluation of the operator S_+ which appears in the master Eq. (12) is essential in order to achieve the multistability mentioned above. The dashed-dotted line in Fig. 3b presents the result obtained by using a procedure similar to that followed in Refs. [56,57], i.e., the operator S_+ is evaluated by considering that in the unitary transformation under the integral in Eq. (13), $H^{\mathrm{c}}_{\mathrm{eff}}$ is restricted to H^{c}_0, i.e., to the atomic plus the control coherent field Ω_{c} terms, and thus ignoring the role of the field which circulates inside the cavity (Ω_{p}) to obtain S_+. The solid line in Fig. 3b presents the result obtained by evaluating S_+ when taking into account the atomic plus the full coherent part of the Hamiltonian, i.e., by considering the control and probe fields (Ω_{c} and Ω_{p}, respectively). It becomes evident that the bistable curves are dramatically modified when considering this second approach, thus in the evaluation of S_+ we must consider the influence of the probe field. The influence of the Rabi frequency of the probe field Ω_{p} on the eigenvalues of the Hamiltonian $H^{\mathrm{c}}_{\mathrm{eff}}$ is depicted in Fig. 3c. Note that one of the eigenvalues is zero due to the two photon resonance condition ($\Delta_{\mathrm{p}} + \Delta_{\mathrm{c}} = 0$), whereas the other two eigenvalues λ_α and λ_β depart from the corresponding eigenvalues of H^{c}_0. Thus the β's in Eq. (19) will depend not only on Ω_{c} but on Ω_{p}. Moreover, numerical simulations carried out show that both the bistability threshold intensity and the width of the bistable region change with phase ϕ, and eventually OB disappears. This behavior opens the possibility of inducing optical switching by varying the relative phase of the control field to the stochastic field. In other words, by keeping constant the input field, it is possible to make the system to jump from a low to a high transmission state with a high contrast between the two states. This behavior is shown in Fig. 3d. There we plot the behavior of the amplitude of the transmitted field when we adiabatically change the phase ϕ while the input field is maintained fixed at a normalized value of $|y| = 70$. The

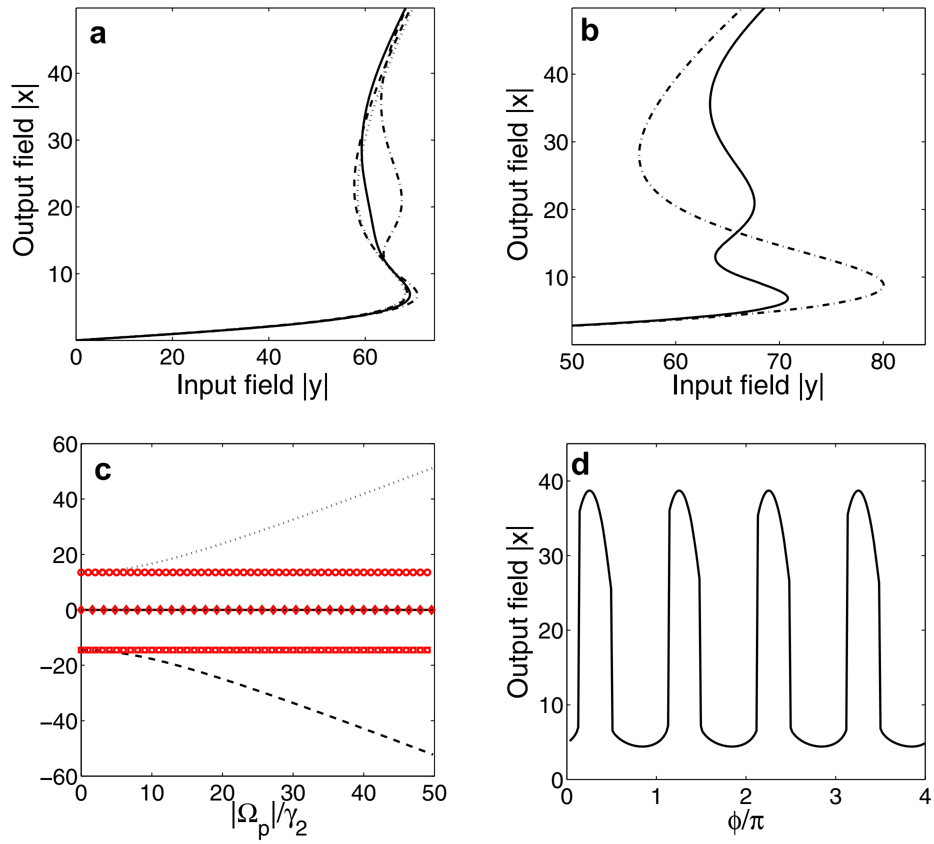

Fig. 3. (a) Output field versus input field for various values of ϕ. The parameters used to produce the curves are: $\Delta_p = -\ \Delta_c = -\gamma_2$, $\Omega_c = 14\gamma_2$, $C = 4 \times 10^3$, $D = 0.5\gamma_2$, $\kappa = 10\gamma_2$, $\delta_s = 0$. Solid line ($\phi = \pi/10$), dashed-dotted line ($\phi = \pi/4$), and dashed line ($\phi = \pi/2$). The dotted line corresponds to the results obtained in the absence of stochastic field. (b) Output field versus input field for the case $\phi = \pi/4$. The dashed-dotted line corresponds to the case where S_+ is computed by using the eigenvalues and eigenstates of H_0^c, while for the solid line curve S_+ is computed using the eigenvalues and eigenstates of H_{eff}^c, i.e., the atomic part of the Hamiltonian and all the coherent fields of the Hamiltonian. (c) Eigenvalues as a function of $|\Omega_p|/\gamma_2$. Dotted line (circles) (λ_α), dashed line (squares) (λ_β), and solid line (diamonds) (λ_γ) are the eigenvalues obtained for $H_{\text{eff}}^c(H_0^c)$. (d) Transmitted normalized field as a function of the phase difference ϕ at a fixed input field $|y| = 70$.

contrast of the output signal between the two states is in the order of *0.8*.

In conclusion, the relative phase can be used as an effective mechanism to control the bistable behavior. This scheme differs from [45] where OB is controlled by the coupling field. Here the parameters of the probe and control field are fixed, and the coherence is modified by the structural properties of the stochastic field which acts as a phase-dependent reservoir. It is this reservoir the responsible for the phase dependence of the bistable response which is unavailable in conventional three-level systems.

Now we turn our attention to the case where $\delta_s \neq 0$, i.e, we will analyze the influence of the detuning δ_s between the angular frequencies of the stochastic field and the coherent control field on the bistable response. Different from the coherent method to manipulate the radiation properties, here we will show that the adjustment of the central frequency of the stochastic field with finite bandwidth can be used to modify the bistable response of the system. The stochastic field influences the dressed atom through terms like $\frac{D\kappa}{\kappa+i\delta_s}$, $\frac{D\kappa}{\kappa+i[\delta_s-(\lambda_\alpha-\lambda_\beta)]}$, among others. When the central frequency of the stochastic field is tuned to $\delta_s - (\lambda_i - \lambda_j)$, the corresponding atomic transition is enhanced and absorption takes place. Fig. 4 presents the input–output curves obtained for various values of δ_s together with the curve corresponding to the absence of stochastic field (solid line). The control field is set to $\Omega_c = 10\gamma_2$, and the parameters of the stochastic field are $\kappa = 10\gamma_2$, and $D = 0.25\gamma_2$. The choice of parameters for the stochastic and control fields guarantees that condition (8) is satisfied. In the absence of stochastic field (see solid line in Fig. 4) we recover the typical bistability curve. However, the addition of a stochastic field produces a dramatic modification of the bistable response: the presence of a stochastic field leads to the appearance of two additional branches for negative and positive values of δ_s. Note that the lower branch of the OB curve is not modified by the action of the stochastic field.

The appearance of multistability at a selected frequency detuning δ_s also depends on the detuning of the probe field (Δ_p). Numerical simulations carried out for $\delta_s = -15\gamma_2$ (not shown) indicate that the multistable behavior is maintained when varying Δ_p in the interval $[-2\gamma_2, 2\gamma_2]$ while keeping the two-photon resonance condition and the rest

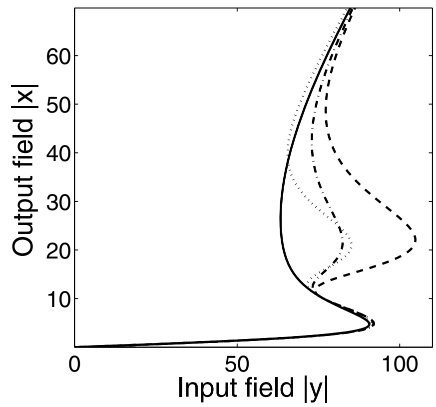

Fig. 4. Output field versus input field for several frequency detunings $\delta_s = -15\gamma_2$ (dashed line), $\delta_s = -10\gamma_2$ (dashed-dotted line) $\delta_s = 15\gamma_2$ (dotted line). The solid line corresponds to the absence of stochastic field. The rest of parameters are: $\Delta_p = -\Delta_c = -\gamma_2$, $\Omega_c = 10\ \gamma_2$, $C = 4 \times 10^3$, $D = 0.25\gamma_2$, $\kappa = 10\ \gamma_2$.

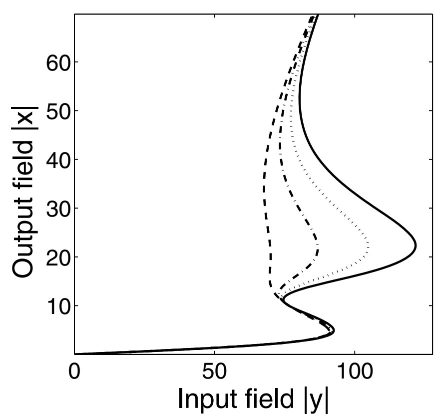

Fig. 5. Output field versus input field for $\Omega_c = 10\ \gamma_2$, $\Delta_p = -\Delta_c = -\gamma_2$, $\delta_s = -15\gamma_2$, $C = 4 \times 10^3$, $\kappa = 10\gamma_2$. $D = 0.05\gamma_2$ (dashed line), $D = 0.15\gamma_2$ (dashed-dotted line), $D = 0.25\gamma_2$ (dotted line), and $D = 0.35\gamma_2$ (solid line).

of parameters as the ones used to produce Fig. 4. The main effect of the change in Δ_p being the reduction of the width of the intermediate branch.

Now we turn our attention to analyze how the strength of the stochastic field D modifies the bistable behavior. Fig. 5 depicts the input–output curves for various values of D and the rest of parameters are those used to produce the dashed line in Fig. 4. For low values of D the upper branch only exhibits two possible states. However, by increasing the value of D, three possible stable states of the output field are achieved for the same value of the input field. The threshold of the intermediate branch increases when increasing D. In addition, the width of the intermediate and upper branches may be altered by changing the value of D. A similar behavior is found numerically when changing the value of κ (not shown).

4. Conclusions

We have analyzed how a stochastic field influences the properties of the steady-state bistable response of a QD semiconductor structure inserted in a ring cavity in the mean field approximation. The QD is modeled as a three-level ladder-type atom which is driven by a control field which does not circulate inside the cavity and allows for all-optical operation of the bistable/multistable response. A perturbative solution of the master equation describing the system has been obtained which provides a physical picture for the stochastic field in terms of its correlation properties. The resulting equations show that the stochastic field acts as an effective bath whose properties may be engineered by changing its central frequency or its phase relative to the phase of the coherent control field. When the central frequency of the stochastic field is equal to that of the control field the system exhibit phase-dependent behavior. This may be used to obtain all-optical multistable operation and phase-switching behavior of the device. We have shown that by adjusting the difference between the angular frequencies of the control field to the stochastic field (δ_s), the upper region of the bistable response is divided into two additional branches which allows for multistable all-optical operation. The existence of these branches, their thresholds and widths may be adjusted by acting on the stochastic field strength D, and other relevant parameters like δ_s and/or Δ_p.

The observed OB behavior in this three-level system inside an optical ring cavity is quite different from the previously studied two-level atomic systems. Because of the induced atomic coherence in such an EIT medium, the absorption, dispersion, and non-linearity are all greatly altered, which make this composite system more complicated and interesting for practical applications. Thus, optical bistability can be achieved in a broad range of parameter space, for example, by controlling the experimental parameters such as intensities and frequencies of the controlling fields. This kind of control was absent from previous experimental two-level systems, where a single field causes the optical pumping and saturation of absorption. Other additional advantage is that the enhanced non-linearity in three-level system due to atomic coherence allows for a considerable reduction of the switching thresholds, which is essential in order to built optical switches at very low intensity levels of light. Moreover, in multilevel systems the dependence of the shift of an optical bistability hysteresis curve on the non-linear phase shift induced by the control field permits that the switching occurs between different hysteresis curves allowing all-optical flip-flop and storage of optical pulse signals.

Acknowledgements

This work has been supported by Projects No. FIS2004-03267 (MEC), PR27/05-14019 (UCM/BSCH) and GR96/06 (UCM/CAM) from Spain.

Appendix A

The derivation of the semiconductor medium equations of motion is carried out in the Heisenberg picture using a

Hamiltonian that contains the contributions from the free-carrier energy, dipole interaction energy with the optical fields, and Coulomb interaction energy among carriers [65,66]

$$H = H_0 + H_{\text{c-f}} + H_{\text{C}}, \tag{A.1}$$

which contains contributions from the free-carrier energy,

$$H_0 = \hbar\sum_n \omega_{en} a_n^+ a_n + \hbar\sum_m \omega_{hm} b_m^+ b_m, \tag{A.2}$$

the carrier-external fields interaction energy,

$$H_{\text{c-f}} = -\sum_{n,m} \left(\mu_{nm} a_n^+ b_m^+ + \mu_{nm}^* b_m a_n\right) E(z,t), \tag{A.3}$$

and the Coulomb interaction energy,

$$H_C = \frac{1}{2}\sum_{n,m,r,s} W_{nm}^{rs} a_r^+ a_s^+ a_m a_n + \frac{1}{2}\sum_{n,m,r,s} W_{nm}^{rs} b_r^+ b_s^+ b_m b_n - \sum_{n,m,r,s} W_{nm}^{rs} a_r^+ b_s^+ b_m a_n. \tag{A.4}$$

In the above equations, a_n and a_n^+ are electron annihilation and creation operators, b_n and b_n^+ are the corresponding operators for holes, ω_n is the free-carrier electron or hole energy, μ_{nm} is the dipole matrix element between states $|n\rangle$ and $|m\rangle$, and the optical field is defined as in Eq. (1) in the paper. Eq. (A.4) contains the Coulomb interaction energy matrix element

$$\begin{aligned} W_{nm}^{rs} &= \int d^2 r_1 \int d^2 r_2 \phi_r^*(r_1)\phi_n(r_1) W(r_2 - r_1)\phi_s^*(r_2)\phi_m(r_2) \\ &= \sum_{q\neq 0} W_q \int d^2 r_1 \phi_r^*(r_1) \mathrm{e}^{-\mathrm{i}q\cdot r_1}\phi_n(r_1) \\ &\quad \times \int d^2 r_2 \phi_s^*(r_2)\mathrm{e}^{-\mathrm{i}q\cdot r_2}\phi_m(r_2), \end{aligned} \tag{A.5}$$

where $\phi_n(r)$ is the dot wave function in the quantum dot plane,

$$W_q = \frac{1}{\epsilon_q}\frac{e^2}{2A\epsilon_b q}, \tag{A.6}$$

is the Fourier transform of the screened Coulomb potential, e is the electron charge, A is the area of the quantum well containing the quantum dots, ϵ_b is the host dielectric constant, and ϵ_q is the dimensionless longitudinal dielectric function.

For a quantum coherence configuration such as it is shown in Fig. 1, the optical field is

$$E^{\mathrm{c}}(z,t) = \frac{1}{2}E_{c0}(t)\mathrm{e}^{-\mathrm{i}(\omega_{\mathrm{c}}t - kz + \phi_{\mathrm{c}})} + E_{p0}\mathrm{e}^{-\mathrm{i}(\omega_{\mathrm{p}}t - kz + \phi_{\mathrm{p}})} + \text{c.c.}, \tag{A.7}$$

with the signal field connecting the $|2\rangle$ and $|3\rangle$ states, and probe field close to resonance to the transition $|1\rangle \leftrightarrow |2\rangle$.

Using the above Hamiltonian and considering only the scheme consisting of three states $|\alpha>$, $|\beta>$ and $|\gamma>$ it is straightforward to derive the equations of motion for the microscopic polarization and populations. The inter-subband polarization is defined as $\sigma_{\alpha\beta} = < b_\beta a_\alpha >$, intra-band polarization as $\sigma_{\beta\gamma} = < b_\gamma a_\beta >$, $n_{e\alpha} =< a_\alpha^+ a_\alpha >$, and $n_\beta =< b_\beta^+ b_\beta >$, are the electron populations, while $n_\gamma =< b_\gamma^+ b_\gamma >$ is the hole population. In the screened HartreeFock limit [65,66], the following coupled equations are obtained:

$$\begin{aligned} \frac{\partial\sigma_{\alpha\beta}}{\partial t} &= -\mathrm{i}(\omega_{\alpha\beta} - \omega_{\mathrm{p}})\sigma_{\alpha\beta} - \mathrm{i}\Omega_{\alpha\beta}\left(n_\alpha + n_\beta - 1\right) + \mathrm{i}\Omega_{\alpha\gamma}\sigma_{\gamma\alpha} + \left(\frac{\partial\sigma_{\alpha\beta}}{\partial t}\right)_{\text{col}}, \\ \frac{\partial\sigma_{\beta\gamma}}{\partial t} &= -\mathrm{i}(\omega_{\beta\gamma} - \omega_{\mathrm{c}})\sigma_{\beta\gamma} - \mathrm{i}\Omega_{\beta\gamma}\left(n_\beta + n_\gamma - 1\right) - \mathrm{i}\Omega_{\alpha\gamma}\sigma_{\alpha\gamma} + \left(\frac{\partial\sigma_{\alpha\beta}}{\partial t}\right)_{\text{col}}, \\ \frac{\partial\sigma_{\alpha\gamma}}{\partial t} &= -\mathrm{i}(\omega_{\alpha\gamma} - \omega_{\mathrm{p}} - \omega_{\mathrm{c}})\sigma_{\alpha\gamma} - \mathrm{i}\Omega_{\alpha\gamma}\sigma_{\alpha\beta} + \mathrm{i}\Omega_{\alpha\beta}\sigma_{\beta\gamma} + \left(\frac{\partial\sigma_{\alpha\beta}}{\partial t}\right)_{\text{col}}, \\ \frac{\partial\sigma_{\alpha\alpha}}{\partial t} &= \mathrm{i}\Omega_{\alpha\beta}\left(\sigma_{\beta\alpha} - \sigma_{\alpha\beta}\right) + \left(\frac{\partial\sigma_{\alpha\alpha}}{\partial t}\right)_{\text{col}}, \\ \frac{\partial\sigma_{\beta\beta}}{\partial t} &= \mathrm{i}\Omega_{\beta\gamma}\left(\sigma_{\gamma\beta} - \sigma_{\beta\gamma}\right) + \left(\frac{\partial\sigma_{\beta\beta}}{\partial t}\right)_{\text{col}}, \end{aligned} \tag{A.8}$$

where both the transition frequency $\omega_{\alpha\beta}$ and the Rabi frequency $\Omega_{\alpha\beta}$ are modified by many-body effects:

$$\begin{aligned} \omega_{\alpha\beta} &= \omega_{\alpha\beta}^{(0)} + \Delta_{\alpha\beta}^{d}, \\ \Omega_{\alpha\beta} &= \frac{\mu_{\alpha\beta}}{2\hbar}E^+ + \Delta_{\alpha\beta}^{nd}. \end{aligned} \tag{A.9}$$

Here, $\omega_{\alpha\beta}^{(0)} = \omega_{en} + \omega_{sm}$ is the unexcited-material transition frequency, $\mu_{\alpha\beta}$ is the dipole matrix element, E^+ is the positive frequency part of Eq. (1) with $z = 0$, and the many-body contributions are grouped into diagonal and non-diagonal terms $\Delta_{\alpha\beta}^{d}$ and $\Delta_{\alpha\beta}^{nd}$, which are given by [66]

$$\Delta_{\alpha\beta}^{d} = -\sum_{\alpha'} W_{\alpha'\alpha'}^{\alpha\alpha} n_{\alpha'} - \sum_{\beta'} W_{\beta'\beta'}^{\beta\beta} n_{\beta'}, \tag{A.10}$$

$$\Delta_{\alpha\beta}^{nd} = \sum_{\alpha'\beta'} W_{\alpha'\beta'}^{\alpha\beta}\sigma_{\alpha'\beta'}, \tag{A.11}$$

where we neglected terms associated with the interaction dot-well. For a discussion on the separation into diagonal and non-diagonal contributions see Ref. [65].

The three first equations in (A.8) is nothing but the polarization components equations with a scattering terms proportional to

$$(n_{e\alpha} + n_{h\beta} - 1) = n_{\mathrm{c}} - n_v, \tag{A.12}$$

which is the inversion of the states α and β. Formally, these equations can be expressed as

$$\frac{\partial\rho}{\partial t} = -\frac{\mathrm{i}}{\hbar}\left[H_{\text{eff}}^{\mathrm{c}}\rho\right] + \left(\frac{\partial\sigma_{\alpha\beta}}{\partial t}\right)_{\text{col}}, \tag{A.13}$$

where the effective Hamiltonian $H_{\text{eff}}^{\mathrm{c}}$ is given by

$$\begin{aligned} H_{\text{eff}}^{\mathrm{c}} &= \hbar\left[\Delta_{\mathrm{p}}\sigma_{\beta\beta} + (\Delta_{\mathrm{p}} + \Delta_{\mathrm{c}})\sigma_{\alpha\alpha}\right] \\ &\quad - \hbar\left(\Omega_{\beta\gamma}\sigma_{\beta\gamma} + \Omega_{\alpha\beta}\sigma_{\alpha\beta} + \text{H.c.}\right), \end{aligned} \tag{A.14}$$

where

$$\begin{aligned}\varDelta_{\mathrm{p}} &= \omega_{\alpha\beta}^{(0)} + \varDelta_{\alpha\beta}^{d} - \omega_{\mathrm{p}},\\ \varDelta_{\mathrm{c}} &= \omega_{\beta\gamma}^{(0)} + \varDelta_{\beta\gamma}^{d} - \omega_{\mathrm{c}},\\ \Omega_{\alpha\beta} &= \Omega_{\mathrm{c}} + \varDelta_{\alpha\beta}^{nd},\\ \Omega_{\beta\gamma} &= \Omega_{\mathrm{p}} + \varDelta_{\beta\gamma}^{nd}.\end{aligned} \tag{A.15}$$

If we assume a situation in which optical excitation is not too strong, the effect of bandgap renormalization can be neglected. Therefore, from the Coulomb interaction we only keep the mutual attraction between electrons and holes. This approximation is justified if the density of generated electron–hole pairs is well below the Mott density [63]. As a result of the above considerations we will assume from now on that the effect of Coulomb interaction is twofold. First, it gives rise to energy shifts which we assume constant. Second, it induces dephasing which we assume is included in phenomenological constant $\gamma_{\alpha\beta}$. With these considerations in mind, the effective Hamiltonian in Eq. (A.14) reduces to the atomic-like hamiltonian for a three-level ladder system as in Eq. (5) of the main paper, where we approximate the polarization dephasing term by

$$\left(\frac{\partial\sigma_{\alpha\beta}}{\partial t}\right)_{\mathrm{col}} = -\gamma_{\alpha\beta}\sigma_{\alpha\beta}, \tag{A.16}$$

where $\gamma_{\alpha\beta}$ is the effective dephasing rate.

Appendix B

The dressed states can be written in terms of the bare states as $(|1\rangle,|2\rangle,|3\rangle)^{\mathrm{tt}} = U(|\alpha\rangle,\ |\beta\rangle,|\gamma\rangle)^{\mathrm{tt}}$, where U stands for the matrix transformation

$$U = \begin{pmatrix} a_{1\alpha} & a_{2\alpha} & a_{3\alpha}\\ a_{1\beta} & a_{2\beta} & a_{3\beta}\\ a_{1\gamma} & a_{2\gamma} & a_{3\gamma}\end{pmatrix}, \tag{B.1}$$

and the coefficients are explicitly given by Eq. (17). The magnitude of interest S_+ in Eq. (13) can be obtained by means of a transform into the basis of the dressed states as follows

$$\begin{aligned}S_+^U = U^{-1}S_+U = D\kappa\int_0^\infty & \mathrm{d}\tau \mathrm{e}^{-(\kappa+\mathrm{i}\delta_s)\tau}(U^{-1}\mathrm{e}^{-\mathrm{i}H_{\mathrm{eff}}^{\mathrm{c}}\tau}U)\\ &\times(U^{-1}\sigma_{32}U)(U^{-1}\mathrm{e}^{\mathrm{i}H_{\mathrm{eff}}^{\mathrm{c}}\tau}U)\\ = D\kappa\int_0^\infty & \mathrm{d}\tau \mathrm{e}^{-(\kappa+\mathrm{i}\delta_s)\tau}\mathrm{e}^{-\mathrm{i}H_0^U\tau}\sigma_{32}^U\mathrm{e}^{\mathrm{i}H_0^U\tau},\end{aligned} \tag{B.2}$$

where

$$\begin{aligned}H_0^U &= U^{-1}H_{\mathrm{eff}}^{\mathrm{c}}U = \lambda_{\alpha\alpha}\sigma_{\alpha\alpha} + \lambda_{\beta\beta}\sigma_{\beta\beta} + \lambda_{\gamma\gamma}\sigma_{\gamma\gamma},\\ \sigma_{32}^U &= U^{-1}\sigma_{32}U = a_{3\alpha}a_{2\alpha}\sigma_{\alpha\alpha} + a_{3\alpha}a_{2\beta}\sigma_{\alpha\beta} + a_{3\alpha}a_{2\gamma}\sigma_{\alpha\gamma}\\ &\quad + a_{3\beta}a_{2\alpha}\sigma_{\beta\alpha} + a_{3\beta}a_{2\beta}\sigma_{\beta\beta} + a_{3\beta}a_{2\gamma}\sigma_{\beta\gamma} + a_{3\gamma}a_{2\alpha}\sigma_{\gamma\alpha}\\ &\quad + a_{3\gamma}a_{2\beta}\sigma_{\gamma\beta} + a_{3\gamma}a_{2\gamma}\sigma_{\gamma\gamma}.\end{aligned} \tag{B.3}$$

Inserting Eq. (B.3) in Eq. (B.2) and taking into account that $\mathrm{e}^{-\mathrm{i}H_0^U\tau}\sigma_{mn}\mathrm{e}^{\mathrm{i}H_0^U\tau} = \sigma_{mn}\mathrm{e}^{-\mathrm{i}(\lambda_m-\lambda_n)\tau}$, we obtain

$$\begin{aligned}S_+^U = D\kappa\int_0^\infty \mathrm{d}\tau \mathrm{e}^{-(\kappa+\mathrm{i}\delta_s)\tau}\big[&\big(a_{3\alpha}a_{2\alpha}\sigma_{\alpha\alpha} + a_{3\beta}a_{2\beta}\sigma_{\beta\beta} + a_{3\gamma}a_{2\gamma}\sigma_{\gamma\gamma}\big)\\ &+ a_{3\gamma}a_{2\alpha}\sigma_{\gamma\alpha}\mathrm{e}^{-\mathrm{i}(\lambda_\gamma-\lambda_\alpha)\tau} + a_{3\gamma}a_{2\beta}\sigma_{\gamma\beta}\mathrm{e}^{-\mathrm{i}(\lambda_\gamma-\lambda_\beta)\tau}\\ &+ a_{3\beta}a_{2\alpha}\sigma_{\beta\alpha}\mathrm{e}^{-\mathrm{i}(\lambda_\beta-\lambda_\alpha)\tau} + a_{3\alpha}a_{2\beta}\sigma_{\alpha\beta}\mathrm{e}^{-\mathrm{i}(\lambda_\alpha-\lambda_\beta)\tau}\\ &+ a_{3\alpha}a_{2\gamma}\sigma_{\alpha\gamma}\mathrm{e}^{-\mathrm{i}(\lambda_\alpha-\lambda_\gamma)\tau} + a_{3\beta}a_{2\gamma}\sigma_{\beta\gamma}\mathrm{e}^{-\mathrm{i}(\lambda_\beta-\lambda_\gamma)\tau}\big].\end{aligned}$$

This integral yields

$$\begin{aligned}S_+^U = D\kappa\Bigg[&\big(a_{3\alpha}a_{2\alpha}\sigma_{\alpha\alpha} + a_{3\beta}a_{2\beta}\sigma_{\beta\beta} + a_{3\gamma}a_{2\gamma}\sigma_{\gamma\gamma}\big)\frac{1}{\kappa+\mathrm{i}\delta_s}\\ &+ a_{3\gamma}a_{2\alpha}\sigma_{\gamma\alpha}\frac{1}{\kappa+\mathrm{i}\big[\delta_s+(\lambda_\gamma-\lambda_\alpha)\big]}\\ &+ a_{3\gamma}a_{2\beta}\sigma_{\gamma\beta}\frac{1}{\kappa+\mathrm{i}\big[\delta_s+(\lambda_\gamma-\lambda_\beta)\big]}\\ &+ a_{3\beta}a_{2\alpha}\sigma_{\beta\alpha}\frac{1}{\kappa+\mathrm{i}\big[\delta_s+(\lambda_\beta-\lambda_\alpha)\big]}\\ &+ a_{3\alpha}a_{2\beta}\sigma_{\alpha\beta}\frac{1}{\kappa+\mathrm{i}\big[\delta_s+(\lambda_\alpha-\lambda_\beta)\big]}\\ &+ a_{3\alpha}a_{2\gamma}\sigma_{\alpha\gamma}\frac{1}{\kappa+\mathrm{i}\big[\delta_s+(\lambda_\alpha-\lambda_\gamma)\big]}\\ &+ a_{3\beta}a_{2\gamma}\sigma_{\beta\gamma}\frac{1}{\kappa+\mathrm{i}\big[\delta_s+(\lambda_\beta-\lambda_\gamma)\big]}\Bigg].\end{aligned} \tag{B.4}$$

The expression for S_+^U can be recast to

$$S_+^U = \begin{pmatrix} a_{3\alpha}a_{2\alpha}\sigma_{\alpha\alpha} + a_{3\beta}a_{2\beta}\sigma_{\beta\beta} + a_{3\gamma}a_{2\gamma}\sigma_{\gamma\gamma}\\ a_{3\gamma}a_{2\alpha}\sigma_{\gamma\alpha}\\ a_{3\gamma}a_{2\beta}\sigma_{\gamma\beta}\\ a_{3\beta}a_{2\alpha}\sigma_{\beta\alpha}\\ a_{3\beta}a_{2\gamma}\sigma_{\beta\gamma}\\ a_{3\alpha}a_{2\gamma}\sigma_{\alpha\gamma}\\ a_{3\beta}a_{2\gamma}\sigma_{\beta\gamma}\end{pmatrix}^{\mathrm{tt}} \begin{pmatrix} 1/(\kappa+\mathrm{i}\delta_s)\\ 1/(\kappa+\mathrm{i}\big[\delta_s+(\lambda_\gamma-\lambda_\alpha)\big])\\ 1/(\kappa+\mathrm{i}\big[\delta_s+(\lambda_\gamma-\lambda_\beta)\big])\\ 1/(\kappa+\mathrm{i}\big[\delta_s+(\lambda_\beta-\lambda_\alpha)\big])\\ 1/(\kappa+\mathrm{i}\big[\delta_s+(\lambda_\alpha-\lambda_\beta)\big])\\ 1/(\kappa+\mathrm{i}\big[\delta_s+(\lambda_\alpha-\lambda_\gamma)\big])\\ 1/(\kappa+\mathrm{i}\big[\delta_s+(\lambda_\beta-\lambda_\gamma)\big])\end{pmatrix}. \tag{B.5}$$

The result (S_+^U) is then transformed back to the bare state basis via $S_+ = US_+^UU^{-1}$, i.e., by transforming each $\sigma_{\eta\chi}$ (η, $\chi = \alpha,\ \beta,\ \gamma$)

$$\sigma_{\eta\chi} = \sum_{i,j=1}^{3} a_{i\eta}a_{j\chi}\sigma_{ij}. \tag{B.6}$$

Then we can obtain the matrix M in Eq. (20), $\vec{\beta} = M\vec{\gamma}$, M being

$$M = \begin{pmatrix}
a_{3\alpha}a_{2\alpha}a_{1\alpha}^2 + a_{3\gamma}a_{2\gamma}a_{1\gamma}^2 + a_{3\beta}a_{2\beta}a_{1\beta}^2 & a_{3\beta}a_{2\alpha}a_{1\beta}a_{1\alpha} & a_{3\beta}a_{2\gamma}a_{1\beta}a_{1\gamma} & a_{3\gamma}a_{2\alpha}a_{1\gamma}a_{1\alpha} & a_{3\alpha}a_{2\gamma}a_{1\alpha}a_{1\gamma} & a_{3\alpha}a_{2\beta}a_{1\alpha}a_{1\beta} & a_{3\gamma}a_{2\beta}a_{1\gamma}a_{1\beta} \\
a_{3\alpha}a_{2\alpha}a_{2\alpha}^2 + a_{3\gamma}a_{2\gamma}a_{2\gamma}^2 + a_{3\beta}a_{2\beta}a_{2\beta}^2 & a_{3\beta}a_{2\alpha}a_{2\beta}a_{2\alpha} & a_{3\beta}a_{2\gamma}a_{2\beta}a_{2\gamma} & a_{3\gamma}a_{2\alpha}a_{2\gamma}a_{2\alpha} & a_{3\alpha}a_{2\gamma}a_{2\alpha}a_{2\gamma} & a_{3\alpha}a_{2\beta}a_{2\alpha}a_{2\beta} & a_{3\gamma}a_{2\beta}a_{2\gamma}a_{2\beta} \\
a_{3\alpha}a_{2\alpha}a_{3\alpha}^2 + a_{3\gamma}a_{2\gamma}a_{3\gamma}^2 + a_{3\beta}a_{2\beta}a_{3\beta}^2 & a_{3\beta}a_{2\alpha}a_{3\beta}a_{3\alpha} & a_{3\beta}a_{2\gamma}a_{3\beta}a_{3\gamma} & a_{3\gamma}a_{2\alpha}a_{3\gamma}a_{3\alpha} & a_{3\alpha}a_{2\gamma}a_{3\alpha}a_{3\gamma} & a_{3\alpha}a_{2\beta}a_{3\alpha}a_{3\beta} & a_{3\gamma}a_{2\beta}a_{3\gamma}a_{3\beta} \\
a_{3\alpha}a_{2\alpha}a_{3\alpha}a_{2\alpha} + a_{3\gamma}a_{2\gamma}a_{3\gamma}a_{2\gamma} + a_{3\beta}a_{2\beta}a_{3\beta}a_{2\beta} & a_{3\beta}a_{2\alpha}a_{3\beta}a_{2\alpha} & a_{3\beta}a_{2\gamma}a_{3\beta}a_{2\gamma} & a_{3\gamma}a_{2\alpha}a_{3\gamma}a_{2\alpha} & a_{3\alpha}a_{2\gamma}a_{3\alpha}a_{2\gamma} & a_{3\alpha}a_{2\beta}a_{3\alpha}a_{2\beta} & a_{3\gamma}a_{2\beta}a_{3\gamma}a_{2\beta} \\
a_{3\alpha}a_{2\alpha}a_{2\alpha}a_{3\alpha} + a_{3\gamma}a_{2\gamma}a_{2\gamma}a_{3\gamma} + a_{3\beta}a_{2\beta}a_{2\beta}a_{3\beta} & a_{3\beta}a_{2\alpha}a_{2\beta}a_{3\alpha} & a_{3\beta}a_{2\gamma}a_{2\beta}a_{3\gamma} & a_{3\gamma}a_{2\alpha}a_{2\gamma}a_{3\alpha} & a_{3\alpha}a_{2\gamma}a_{2\alpha}a_{3\gamma} & a_{3\alpha}a_{2\beta}a_{2\alpha}a_{3\beta} & a_{3\gamma}a_{2\beta}a_{2\gamma}a_{3\beta} \\
a_{3\alpha}a_{2\alpha}a_{1\alpha}a_{2\alpha} + a_{3\gamma}a_{2\gamma}a_{1\gamma}a_{2\gamma} + a_{3\beta}a_{2\beta}a_{1\beta}a_{2\beta} & a_{3\beta}a_{2\alpha}a_{1\beta}a_{2\alpha} & a_{3\beta}a_{2\gamma}a_{1\beta}a_{2\gamma} & a_{3\gamma}a_{2\alpha}a_{1\gamma}a_{2\alpha} & a_{3\alpha}a_{2\gamma}a_{1\alpha}a_{2\gamma} & a_{3\alpha}a_{2\beta}a_{1\alpha}a_{2\beta} & a_{3\gamma}a_{2\beta}a_{1\gamma}a_{2\beta} \\
a_{3\alpha}a_{2\alpha}a_{2\alpha}a_{1\alpha} + a_{3\gamma}a_{2\gamma}a_{2\gamma}a_{1\gamma} + a_{3\beta}a_{2\beta}a_{2\beta}a_{1\beta} & a_{3\beta}a_{2\alpha}a_{2\beta}a_{1\alpha} & a_{3\beta}a_{2\gamma}a_{2\beta}a_{1\gamma} & a_{3\gamma}a_{2\alpha}a_{2\gamma}a_{1\alpha} & a_{3\alpha}a_{2\gamma}a_{2\alpha}a_{1\gamma} & a_{3\alpha}a_{2\beta}a_{2\alpha}a_{1\beta} & a_{3\gamma}a_{2\beta}a_{2\gamma}a_{1\beta} \\
a_{3\alpha}a_{2\alpha}a_{1\alpha}a_{3\alpha} + a_{3\gamma}a_{2\gamma}a_{1\gamma}a_{3\gamma} + a_{3\beta}a_{2\beta}a_{1\beta}a_{3\beta} & a_{3\beta}a_{2\alpha}a_{1\beta}a_{3\alpha} & a_{3\beta}a_{2\gamma}a_{1\beta}a_{3\gamma} & a_{3\gamma}a_{2\alpha}a_{1\gamma}a_{3\alpha} & a_{3\alpha}a_{2\gamma}a_{1\alpha}a_{3\gamma} & a_{3\alpha}a_{2\beta}a_{1\alpha}a_{3\beta} & a_{3\gamma}a_{2\beta}a_{1\gamma}a_{3\beta} \\
a_{3\alpha}a_{2\alpha}a_{3\alpha}a_{1\alpha} + a_{3\gamma}a_{2\gamma}a_{3\gamma}a_{1\gamma} + a_{3\beta}a_{2\beta}a_{3\beta}a_{1\beta} & a_{3\beta}a_{2\alpha}a_{3\beta}a_{1\alpha} & a_{3\beta}a_{2\gamma}a_{3\beta}a_{1\gamma} & a_{3\gamma}a_{2\alpha}a_{3\gamma}a_{1\alpha} & a_{3\alpha}a_{2\gamma}a_{3\alpha}a_{1\gamma} & a_{3\alpha}a_{2\beta}a_{3\alpha}a_{1\beta} & a_{3\gamma}a_{2\beta}a_{3\gamma}a_{1\beta}
\end{pmatrix}. \tag{B.7}$$

References

[1] L.A. Lugiato, in: E. Wolf (Ed.), Progress in Optics, vol. 21, North-Holland, Amsterdam, 1984.
[2] H.M. Gibbs, S.L. McCall, T.N.C. Venkatesan, Phys. Rev. Lett. 3 (1976) 1135.
[3] L.A. Orozco, H.J. Kimble, A.T. Rosenberger, L.A. Lugiato, M.L. Asquini, M. Brambilla, L.M. Narducci, Phys. Rev. A 39 (1989) 1235.
[4] T. Ackemann et al., Phys. Rev. A 56 (1997) 2321.
[5] J. Gripp, S.L. Mielke, L.A. Orozco, Phys. Rev. A 56 (1997) 3262.
[6] L.A. Orozco, A.T. Rosenberger, H.J. Kimble, Phys. Rev. Lett. 53 (1984) 2547;
G. Rempe et al., Phys. Rev. Lett. 67 (1991) 1727;
G.T. Foster et al., Phys. Rev. A 66 (2002) 033807.
[7] F.T. Arecchi, J. Kurmann, A. Politi, Opt. Commun. 44 (1983) 421.
[8] E. Giacobino, Opt. Commun. 56 (1985) 249.
[9] M. Kitano, T. Yabuzaki, T. Ogawa, Phys. Rev. Lett. 46 (1981) 926.
[10] S. Cecchi, G. Giusfredi, E. Petriella, P. Salieri, Phys. Rev. Lett. 49 (1982) 1928.
[11] D.F. Walls, P. Zoller, Opt. Commun. 34 (1980) 260.
[12] D.F. Walls, P. Zoller, M.L. Steÿn-Ross, IEEE J. Quantum Electron. QE-17 (1981) 380.
[13] W. Harshawardhan, G.S. Agarwal, Phys. Rev. A 53 (1996) 1812.
[14] H. Wang, D.J. Goorskey, W.H. Burkett, M. Xiao, Opt. Lett. 25 (2000) 1732.
[15] H. Wang, D.J. Goorskey, M. Xiao, Phys. Rev. A 65 (2001) 011801.
[16] H. Wang, D.J. Goorskey, M. Xiao, Opt. Lett. 27 (2002) 1354.
[17] A. Joshi, A. Brown, H. Wang, M. Xiao, Phys. Rev. A 67 (2003) 041801.
[18] A. Joshi, A. Brown, H. Wang, M. Xiao, Phys. Rev. A 70 (2004) 041802(R).
[19] A. Joshi, A. Brown, H. Wang, M. Xiao, Phys. Rev. Lett. 91 (2003) 143904.
[20] H. Chang, H. Wu, C. Xie, H. Wang, Phys. Rev. Lett. 93 (2004) 213901.
[21] M.A. Antón, O.G. Calderón, S. Melle, I. Gonzalo, F. Carreño, Opt. Commun. 268 (2006) 146.
[22] I. Novikova, A.S. Zibrov, D.F. Phillips, A. André, R.L. Walsworth, Phys. Rev. A 69 (2004) 061802.
[23] A. Joshi, W. Yang, M. Xiao, Opt. Lett. 30 (2005) 905.
[24] A. Joshi, W. Yang, M. Xiao, Phys. Lett. A 315 (2003) 203.
[25] M.A. Antón, O.G. Calderón, J. Opt. B: Quantum Semiclass. Opt. 4 (2002) 91.
[26] M.A. Antón, O.G. Calderón, F. Carreño, Phys. Lett. A 311 (2003) 297.
[27] S.Q. Gong, S.D. Du, Z.Z. Xu, Phys. Lett. A 226 (1997) 293.
[28] D. Cheng, C. Liu, S. Wang, S.Q. Gong, Opt. Commun. 263 (2006) 111.
[29] P.C. Ku, F. Sedgwick, C.J. Chang-Hasnain, P. Palinginis, T. Li, H. Wang, S.W. Chang, S.L. Chuang, Opt. Lett. 29 (2004) 2291.
[30] P. Palinginis, F. Sedgwick, S. Crankshaw, M. Moewe, C. Chang-Hasnain, Opt. Express 13 (2005) 9909.
[31] H. Su, S.L. Chuang, Opt. Lett. 31 (2006) 271.
[32] M. Phillips, H. Wang, Phys. Rev. Lett. 89 (2002) 186401.
[33] M. Phillips, H. Wang, Opt. Lett. 28 (2003) 831.
[34] G.B. Serapiglia, E. Paspalakis, C. Sirtori, K.L. Vodopyanov, C.C. Phillips, Phys. Rev. Lett. 84 (2003) 1019.
[35] L. Silvestri, F. Bassani, G. Czajkowski, B. Davoudi, Eur. Phys. J. B 27 (2002) 89.
[36] A.A. Belyanin, F. Capasso, V.V. Kocharovsky, Vl.V. Kocharovsky, M.O. Scully, Phys. Rev. A 63 (2001) 053803.
[37] P.C. Ku, C.J. Chang-Hasnain, S.L. Chuang, Electron. Lett. 38 (2002) 1581.
[38] J. Kim, S.L. Chuan, P.C. Ku, C.J. Chang-Hasnain, J. Phys.: Condens. Matter 16 (2004) S3727.
[39] S.F. Yelin, P.R. Hemmer, Phys. Rev. A 66 (2002) 013803.
[40] H. Schmidt, K.L. Campman, A.C. Gossard, A. Imamoglu, Appl. Phys. Lett. 70 (1997) 3455.
[41] H. Schmidt, R.J. Ram, Appl. Phys. Lett. 76 (2000) 3173.
[42] J.H. Wu, J.Y. Gao, J.H. Xu, L. Silvestri, M. Artoni, G.C. LaRocca, F. Bassani, Phys. Rev. Lett. 95 (2005) 057401.
[43] B.S. Ham, Appl. Phys. Lett. 78 (2001) 3382.
[44] W. Pötz, Phys. Rev. B 71 (2005) 125331.
[45] A. Joshi, M. Xiao, Appl. Phys. B 79 (2004) 65.

[46] J.H. Li, Opt. Commun. 274 (2007) 366.
[47] J.H. Li, Phys. Rev. B 75 (2007) 155329.
[48] R. Bonifacio, L.A. Lugiato, in: L. Mandel, E. Wolf (Eds.), Coherence and Quantum Optics IV, Plenum, NY, 1978, p. 249.
[49] R. Bonifacio, L.A. Lugiato, Phys. Rev. Lett. 40 (1978) 1023.
[50] R. Bonifacio et al., Phys. Rev. A 18 (1978) 2266.
[51] P. Hanggi et al., Phys. Rev. A 22 (1980) 671.
[52] A.P. Saiko, Quantum Electron. 28 (1998) 251.
[53] L. Zhang, L. Cao, D. Wu, Phys. Rev. A 77 (2008) 015801.
[54] P. Zhou, S. Swain, Phys. Rev. Lett. 82 (1999) 2500.
[55] S.Q. Gong, S.D. Du, Z.Z. Xu, S.H. Pan, Phys. Lett. A 222 (1996) 237.
[56] X.M. Hu, Z.Z. Xu, J. Opt. B: Quantum Semiclass. Opt. 3 (2001) 35.
[57] K.I. Osman, S.S. Hassan, Eur. Phys. J. D 38 (2006) 537.
[58] C.J. Chang-Hasnain, P.C. Ku, J. Kim, S.L. Chuang, Proc. IEEE 91 (2003) 1884.
[59] J. Kim, S.L. Chuang, P.C. Ku, C.J. Chang-Hasnain, J. Phys.: Condens. Matter. 16 (2004) S3727.
[60] P.K. Nielsen, H. Thyrrestrup, J. Mørk, B. Tromborg, Opt. Express 15 (2007) 6396.
[61] P. Borri, W. Langbein, S. Schneider, U. Woggon, R.L. Sellin, D. Ouyang, D. Bimberg, Phys. Rev. Lett. 87 (2001) 157401.
[62] H.C. Schnneider, W.W. Chow, M.C. Phillips, Phys. Rev. B 64 (2001) 115315.
[63] M. Lindberg, S.W. Koch, Phys. Rev. B 38 (1988) 3342.
[64] N.G. van Kampen, Stochastics Process in Physics and Chemistry, North-Holland, Amsterdan, 1981.
[65] H. Haug, S.W. Koch, Quantum Theory of the Optical and Electronic Properties of Semiconductors, World Scientific, 2004 (Chapter 12).
[66] W.W. Chow, H.C. Schnneider, M.C. Phillips, Phys. Rev. A 68 (2003) 053802.